Images of oligomeric Kvβ2, a modulatory subunit of potassium channels

Rika van Huizen[a,1], Daniel M. Czajkowsky[b,1], Dan Shi[b], Zhifeng Shao[b], Min Li[a,*]

[a] *Department of Physiology and Department of Neuroscience, The Johns Hopkins University School of Medicine, 725 North Wolfe Street, WBSB 216, Baltimore, MD 21205, USA*

[b] *Department of Molecular Physiology, University of Virginia School of Medicine, Charlottesville, VA 22908, USA*

Received 2 July 1999; received in revised form 19 July 1999

Abstract The Shaker type voltage-gated potassium (K^+) channel consists of four pore-forming Kvα subunits. The channel expression and kinetic properties can be modulated by auxiliary hydrophilic Kvβ subunits via formation of heteromultimeric Kvα-Kvβ complexes. Because each $(Kv\alpha)_4$ could recruit more than one Kvβ subunit and different Kvβ subunits could potentially interact, the stoichiometry of α-β and β-β complexes is therefore critical for understanding the functional regulation of Shaker type potassium channels. We expressed and purified Kvβ2 subunit in Sf9 insect cells. The purified Kvβ2, examined by atomic force and electron microscopy techniques, is found predominately as a square-shaped tetrameric complex with side dimensions of 100×100 Å^2 and height of 51 Å. Thus, Kvβ2 is capable of forming a tetramer in the absence of pore-forming α subunits. The center of the Kvβ2 complex was observed to be the most heavily stained region, suggesting that this region could be part of an extended tubular structure connecting the inner mouth of the ion permeation pathway to the cytoplasmic environment.

Key words: Potassium channel; Subunit assembly; Auxiliary subunit

1. Introduction

Ion channels are oligomeric proteins that are usually composed of several classes of proteins. The pore-forming subunits define the ion permeation pathway and control much of the channel gating properties. Structural studies of these proteins, including the prokaryotic KcsA potassium channel [1] and the acetylcholine (ACh) receptor [2], have provided important insights into the structure and function. As regulatory modules, auxiliary subunits for a variety of ion channels have also been found. Although their functional roles in subunit assembly and modulation have been increasingly recognized, their structure and stoichiometry have not been studied by biophysical techniques (see reviews by [3–5]).

Voltage-gated Shaker type K^+ channels are composed of at least two types of subunits, pore-forming transmembrane Kvα subunits and hydrophilic cytoplasmic Kvβ subunits. Kvα subunits consist of six putative transmembrane segments with both amino (N)- and carboxy (C)-termini positioned on the cytoplasmic side [6,7]. When expressed individually, most Kvα subunits form functional K^+ channels. The expression level and inactivation kinetics can be modulated by coexpression of Kvβ subunits in heterologous systems [8,9]. Genetic mutation of the *hyperkinetics* (Hk) protein, a Kvβ subunit in *Drosophila*, causes significant muscle dysfunction [10]. Homologous Kvβ-like proteins have been found in a variety of species including plants, squid, *Drosophila*, and mammals. At least nine genes encoding various Kvβ subunits have been isolated. They share a highly conserved core region at the C-terminal portion, but the N-terminal portions of the β subunits vary significantly in both length and sequence (see a recent review [5]).

Shaker type potassium channels are assembled as Kvα tetramers as determined by toxin binding and kinetic analyses [11] and by electron microscopy studies of purified Shaker protein [12]. The formation of the $(Kv\alpha)_4$ complex is mediated by associations between the cytoplasmic amino-terminal T1 (or NAB) domains [13–15]. The interaction with Kvβ subunits occurs through associations between the T1 domain of α subunits and the conserved core regions of Kvβ subunits [16,17]. Crystallographic studies have shown that the T1 domain forms a four-fold symmetric tetrameric complex [18]. Thus, the completely assembled four-fold symmetric Kvα tetramer could contain as many as four sites for interaction with Kvβ proteins. Among the cloned Kvβ subunits, mammalian Kvβ1 and Kvβ2 are the ones that have been studied most extensively: Kvβ1 induces or accelerates fast inactivation, whereas Kvβ2 does not exhibit significant effects on channel kinetics [8]. Yeast two-hybrid genetic studies have shown that Kvβ2 has the ability to interact homomultimerically or heteromultimerically with Kvβ1 [19]. In transfected cells, coexpression of Kvβ1 and Kvβ2 subunits abolishes the Kvβ1-mediated fast inactivation, which presumably results from the formation of Kvβ heteromultimers and/or competition for the binding sites of Kvα subunits [19,20]. However, there is as yet no direct evidence that Kvβ subunits self-associate physically to form an oligomeric complex. Because the composition and stoichiometry of the α-β complex could ultimately determine the kinetics and gating properties of the K^+ channel, imaging a purified Kvβ subunit may provide important insights into the mechanism by which these subunits affect channel function. In this study, we expressed and purified the Kvβ2 subunit in the absence of Kvα subunits and visualized the purified protein using atomic force and electron microscopy. The images of the oligomeric Kvβ2 complexes have provided important information on the cytoplasmic dimensions of Shaker type potassium channels.

2. Materials and methods

2.1. Construction of Kvβ2 baculoviruses

Full-length rat Kvβ2 [16] was amplified by PCR and cloned into the *Eco*RI and *Xho*I sites of pBlueBacHis2B (Invitrogen, CA) to generate the plasmid pBlueBacHis2B-Kvβ2. When expressed, the recombinant Kvβ2 contains an extra 37 amino acids at its N-terminus (Fig. 1A), including a hexahistidine tag, an antibody epitope, and an enteroki-

*Corresponding author. Fax: (1) (410) 614-1001.
E-mail: minli@jhmi.edu

[1] These two authors contributed equally to the work.

0014-5793/99/$20.00
PII: S0014-5793(99)01021-2

nase protease cleavage site. Sf9 cells were cotransfected with pBlueBacHis2B-Kvβ2 and linearized AcMNPV genomic DNA using cationic liposomes (Invitrogen, CA); recombinant plaques were identified using 5-bromo-4-chloro-3-indolyl β-D-galactopyranoside staining. Viral stocks were prepared and amplified using standard methods provided by the manufacturer.

2.2. Expression and purification of Kvβ2

Kvβ2 was expressed by infecting Sf9 cells with recombinant baculoviruses. In a typical purification, $4–8\times10^8$ Sf9 insect cells, in 400 ml of Grace's medium that contained 3.3 mg/ml lactalbumin hydrolysate, 3.3 mg/ml yeastolate, 20 μg/ml gentamicin, 0.1% Pluronic F-68, and 10% fetal calf serum, were infected with the His-Kvβ2 viruses at an MOI (multiplicity of infection) of 5–10. After shaking at 100 rpm in a 2500 ml low foam culture flask for 48 h at 27°C, cells were harvested by centrifugation at $2000\times g$ and pelleted cells were stored at −80°C prior to use. For purification, cells were thawed, resuspended in a lysis buffer [50 mM NaH_2PO_4 (pH 8.0), 300 mM NaCl, 10 mM imidazole and 5 mM 2-mercaptoethanol] and lysed by sonication for 2 min on a 30% duty cycle, microprobe setting 6 (model 250/450 Sonifer, Branson Ultrasonics Corporation, NJ). All subsequent steps were carried out at 4°C. The total cell lysates were collected after centrifugation at $12\,000\times g$ for 15 min to remove cell debris. His-tagged proteins were purified by incubation with the crude cell lysate with 1 ml Probond nickel-chelated resin (Invitrogen, CA). After washing the column with a buffer containing 50 mM NaH_2PO_4 (pH 8.0), 300 mM NaCl, 20 mM imidazole and 5 mM 2-mercaptoethanol, Kvβ2 was eluted with the buffer supplemented with 250 mM imidazole.

2.3. Gel filtration chromatography

Protein in 50 mM NaH_2PO_4 (pH 8.0), 300 mM NaCl, 250 mM imidazole, and 5 mM 2-mercaptoethanol was separated by FPLC on Superdex-200 in a running buffer containing 50 mM NaH_2PO_4 (pH 8.0), 300 mM NaCl and 5 mM 2-mercaptoethanol. Generally, 50 μg His-Kvβ2 in 200 μl of the running buffer was loaded. The column was developed at a flow rate of 0.5 ml/fraction/min.

2.4. Microscopy

Typically, for atomic force microscopy (AFM), the experimental procedures were essentially identical to a published protocol [21]. Briefly, a solution of purified His-Kvβ2 subunits (at 10 μg/ml) in 10 mM Tris-HCl (pH 7.2), 150 mM NaCl was incubated on freshly cleaved mica for 30 min at room temperature. Following extensive washing, the sample was imaged, in the same buffer, using a Nanoscope II atomic force microscope (Digital Instruments, Santa Barbara, CA). All images were acquired in the contact mode using oxide-sharpened 'twin tip' Si_3N_4 cantilevers with a spring constant of 0.06 N/m at a typical scan rate of 9 Hz and applied force of ∼0.1 nN. The piezoscanner was calibrated with mica and the cholera toxin β subunit [22]. Lateral dimensions of the His-Kvβ2 subunits were determined from full width at half height using Nanoscope III software.

For electron microscopy (EM), a solution of His-Kvβ2 subunits (at ∼15 μg/ml) in a buffer containing 10 mM Tris-HCl (pH 8.0), 150 mM NaCl, 1 mM EDTA and 5 mM 2-mercaptoethanol, was applied to glow discharged carbon-coated grids. After a brief period of incubation, the sample was stained with 2% uranyl acetate and then imaged with a Philips CM12 electron microscope. To determine the lateral dimensions, EM images were converted into Nanoscope III files, and measurements were made of the full width at half intensity with Nanoscope III software.

3. Results and discussion

The Kvβ2 subunit is the most abundant isoform found in native tissues. However, its absolute amount and potential heterogeneity via oligomerization with other proteins render large-scale purification difficult. To facilitate structural studies, we chose to express rat Kvβ2 cDNA in Sf9 cells using a baculovirus system containing a His tag (Fig. 1A). The tagged fusion protein was soluble and affinity-purified on a nickel column. The purified material yielded a single band on Coomassie-stained SDS-polyacrylamide gel (Fig. 1B, lane 3) with

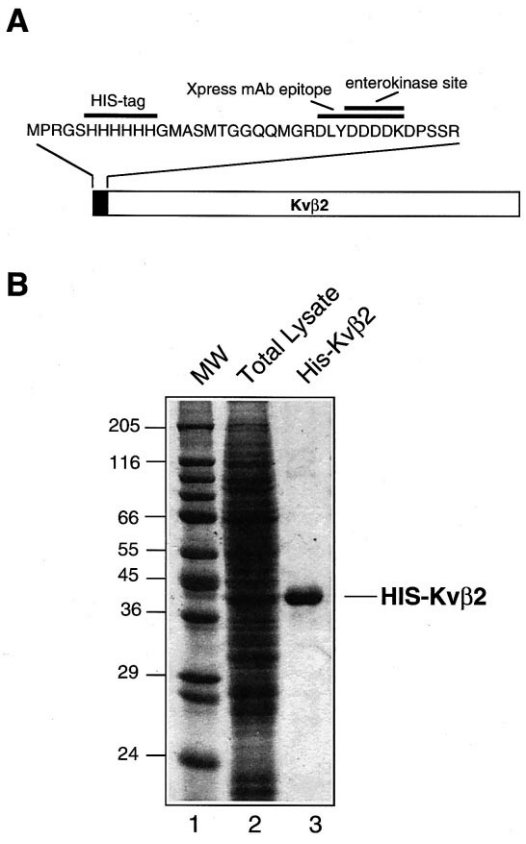

Fig. 1. Expression and purification of Kvβ2. A: A diagram of His-tagged Kvβ2 fusion protein. B: The His-tagged Kvβ2 (His-Kvβ2) protein produced in Sf9 insect cells was affinity purified from crude cell lysates. The cell lysate (lane 2) and the purified Kvβ2 (lane 3) were separated by polyacrylamide gel (12%) and visualized by Coomassie stain.

an apparent molecular weight of 37 kDa, consistent with the molecular weight of the native Kvβ2 [23].

To investigate the hydrodynamic properties of Kvβ2, the purified His-Kvβ2 was separated on a Superdex-200 gel filtration column by FPLC. The A_{280} chromatogram of the Superdex-200 revealed a single peak, corresponding to Kvβ2 as determined by SDS-PAGE (Fig. 2B). Using molecular weight standards, the Stoke's radius of His-Kvβ2 was determined to be 65.4 Å (Fig. 2A), which is considerably greater than a 37 kDa monomer. Therefore, in solution, His-Kvβ2 is oligomeric.

To directly determine the stoichiometry of the His-Kvβ2 complex, the purified protein was examined by EM and AFM. Electron micrographs of negatively stained His-Kvβ2 reproducibly showed square-shaped complexes, approximately 100×100 Å^2, oriented with the four-fold axis normal to the supporting substrate (Fig. 3A,B). Each of the four individual globular 'domains' of the complex is 37 ± 7 Å ($n=211$) in diameter. Between adjacent domains there is a 23 ± 7 Å ($n=109$) densely stained gap. The most heavily stained region was frequently found to be the center of the complex with a cross dimension of 36 ± 8 Å ($n=48$), suggesting that there may be either a central vestibule or, more likely, a central aqueous pore formed by the assembled His-Kvβ2 subunits.

If each His-Kvβ2 subunit is an ellipsoid with a mass density of 1.23 Å^3/Da (a specific volume calculated for the acetylcho-

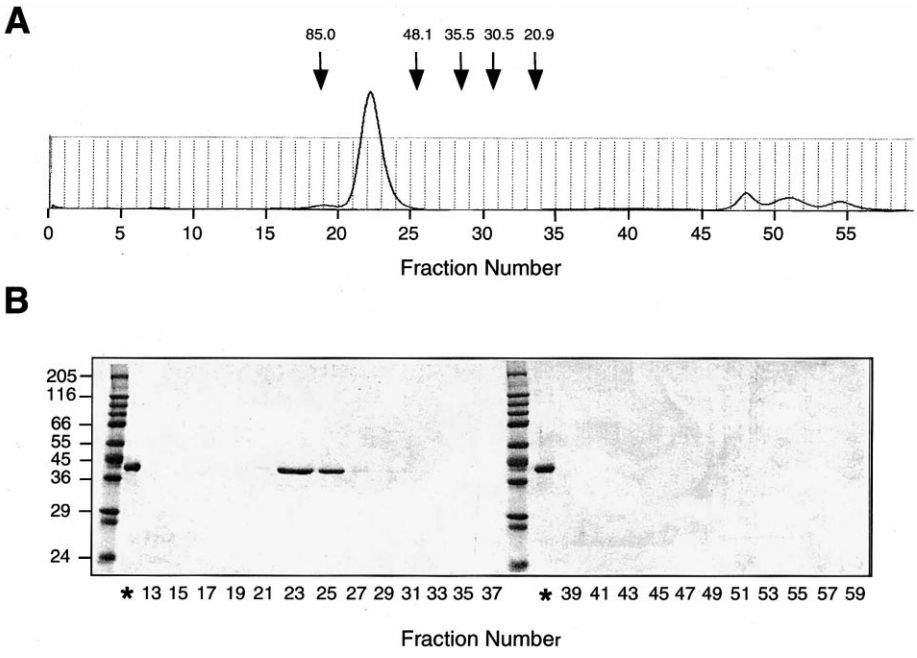

Fig. 2. Purified Kvβ2 proteins are oligomers. A: Gel filtration fractionation of His-Kvβ2. Superdex-200 was used to separate the purified protein and A_{280} chromatogram profiles are shown. Protein Stoke's radius standards (in Å) are thyroglobin (85.0), aldolase (48.1), bovine serum albumin (35.5), chicken ovalbumin (30.5), and chymotrypsinogen (20.9). Their migration positions on Superdex-200 are marked by arrows. B: SDS-PAGE analysis of proteins in fractions after Superdex-200 (FPLC) separation. Lanes marked with an asterisk are the starting material. Numbers under each lane indicate the corresponding fractions in Superdex-200 (B). Molecular weight (in kDa) standards are shown on the left.

line receptor [24]), the dimensions determined from the EM images would predict that such a tetrameric assembly of Kvβ2 subunits would have a total height of ~46 Å. To directly determine the height of the complex, purified His-Kvβ2 was adsorbed onto a mica substrate and examined by AFM, a technique that has been used to determine the height of macromolecules [22,25]. Consistent with the EM observations, square-shaped complexes with a side length of ~100 Å were also routinely observed in the somewhat densely packed sample (Fig. 3D). Each of the four globular domains in the complex is 41 ± 10 Å (n = 266) in diameter with a 19 ± 4 Å (n = 136) groove separating adjacent domains. The total height of the complex, measured from the top of the protein to the mica substrate, in these topographs is 51 ± 6 Å (n = 292), remarkably close to the value predicted above. Taken together, the size and symmetry of the complex determined from both EM and AFM studies clearly indicate that purified His-Kvβ2 predominantly forms tetramers.

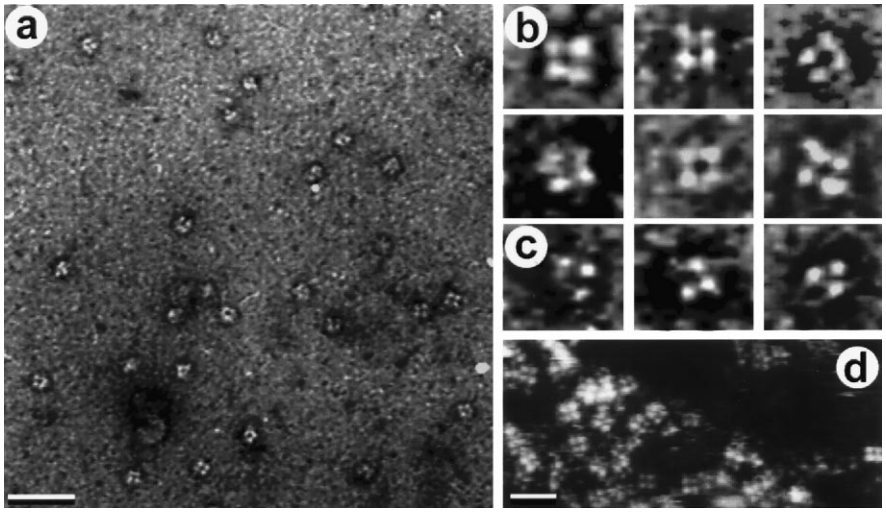

Fig. 3. Images from electron and atomic force microscopy show that purified His-Kvβ2 subunits form tetramers. a: Negative-stain electron microscopy shows that the His-Kvβ2 complex is oriented predominantly with the four-fold symmetry axis perpendicular to the support film, resulting in a square-shaped appearance. (Bar = 500 Å.) b: A panel of six individual His-Kvβ2 complexes was collected from EM. Each image is 240×280 Å^2. Each complex contains four globular domains, corresponding to each subunit. c: A panel of three individual His-Kvβ2 oligomers containing only three subunits. d: Purified His-Kvβ2 visualized by AFM which also reveal square-shaped complexes. The total height of the complex determined from these topographs is ~50 Å. (Bar = 250 Å.)

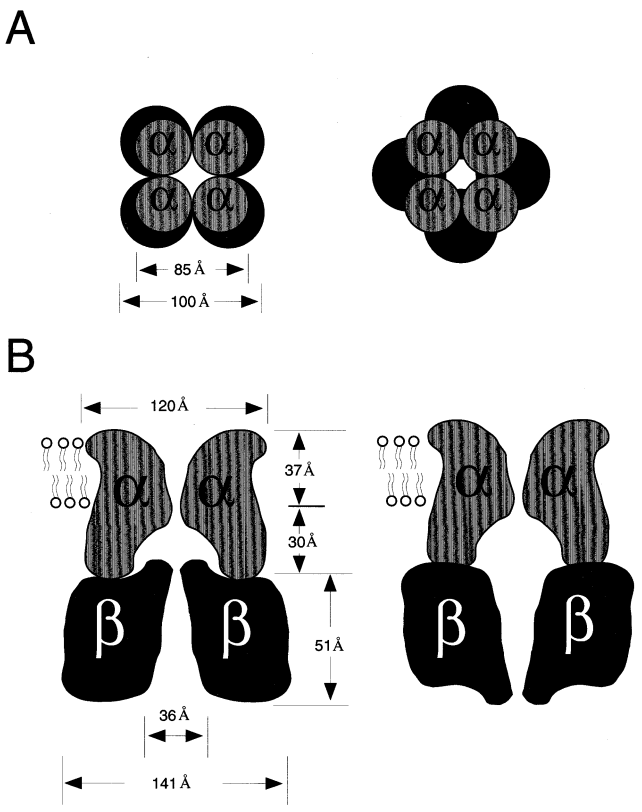

Fig. 4. Dimensions of the $\alpha_4\beta_4$ potassium channel complex. A: Direct (left) and alternative (right) models of $\alpha_4\beta_4$ complexes. The side dimension of α_4 is taken from the EM investigation [12]. The β_4 side dimension of 100 Å is from the present study. B: A side view, along the diagonal of the $\alpha_4\beta_4$ complex. Total height of α_4 is 67 Å that is derived from the height of the KcsA transmembrane core region (37 Å [1]) and the height of T1 domain (30 Å [18]). The height of β_4 is 51 Å (from the present study). The inner and outer cross dimensions of α_4 and β_4 are calculated from the side dimensions. It should be noted that the dimensions obtained from different domains or subunits may not be necessarily additive. The native $\alpha_4\beta_4$ could have deviated dimension due to, for example, interaction-induced conformation changes. The narrow pore of $\beta_4$is based on the crystal structure of $(K\nu\beta)_4$ [33].

It should be noted, however, that complexes with only three domains were also observed by both EM and AFM (~20%, Fig. 3C). The domains in these trimeric complexes were of the same size as those in the tetramers, and moreover, were arranged in the form of a right-angle triangle, suggesting that these three-domain complexes represent intermediates in the process of assembly or disassembly of the His-Kvβ2 tetramer. The observed trimeric complex is consistent with the notion that the four-fold symmetric complex is formed by sequential assembly of four individual subunits as suggested by the earlier studies [20].

Kvβ2 is the most abundant subunit in rat brain and early hydrodynamic studies suggested that the native Kvα1.2-Kvβ2 complex in bovine brain is consistent with an α/β ratio of 1:1 which led to the prediction of $\alpha_4\beta_4$ stoichiometry [23]. The most pronounced activity of Kvβ subunits is the induction of fast inactivation by Kvβ1 subunits [8]. Functional tests in heterologous systems suggested that Kvβ1 could incrementally regulate channel activity. The gradual increase of the inactivation rate induced by increasing the level of Kvβ1 expression suggests a functional stoichiometry of $\alpha_4\beta_n$, where n was thought to equal 0–4 depending upon the Kvβ1 expression level [20]. In contrast, Kvβ2 itself does not exert obvious effects on Kvα subunit inactivation. However, when Kvβ1 and Kvβ2 are coexpressed in tissue culture cells, Kvβ2 could completely inhibit the fast inactivation induced by Kvβ1 [19]. Although the binding affinity between individual Kvα subunits and Kvβ subunits has not been determined, the formation of tetrameric Kvβ2 complex creates multivalent interaction that significantly tightens the $\alpha_4\beta_4$ complex. Such multivalent interaction may improve the on-rate of α-β association during the early stage of channel assembly and/or reduce the off-rate for the assembled α-β complex on the cell membrane.

The shape and symmetry of the Kvβ2 oligomer suggests that the four-fold axis of the Kvβ2 tetramer is aligned with the central pore of the K^+ channel during α-β interaction. The lateral size of the Kvβ2 tetramer is slightly larger than the dimensions of the α subunits of the Shaker α_4 tetramer determined by EM (side length of 80–85 Å [12]) and the tetramer of the T1 domain determined by X-ray crystallography (side length 65–70 Å [18]). During preparation of this work, an independent study reported crystal structure of Kvβ2 with approximate dimensions of $90\times90\times40$ Å [33]. Except slightly smaller in overall size, the relative dimensions are in general agreement with AFM and EM measurements reported here. Although the angular orientation of the β subunits relative to the α subunits in the $\alpha_4\beta_4$ complex is not known, the lateral dimensions measured here indicate that the outer central cavity of the Kvβ2 tetramer has a dimension of ~36 Å. Thus, the 100×100 Å lateral surface of Kvβ2 tetramer should effectively cover the outer surface of the T1 tetramer. Surprisingly, the crystal structure of the Kvβ2 tetramer has a narrow pore (~5 Å). It is not known whether the Kvα-Kvβ interaction induces widening of the narrow pore. In addition, it would be interesting to determine the orientation by which $(K\nu\beta2)_4$ is docked to the $(K\nu\alpha)_4$ complex (Fig. 4). Thus, it is likely that binding of the Kvβ2 tetramer to the cytoplasmic surface of the T1 tetramer excludes other possible interactions between the N-terminal surface of Kvα tetramer and other soluble proteins.

A surprising characteristic of the Kvβ2 tetramer is its rather large total height (~51 Å). If the Kvβ2 complex was only mainly interacting with the α subunits, it might be expected that the Kvβ2 tetramer would be only as high as one or two layers of secondary structures (~10–20 Å). Instead, there is apparently a large portion of the Kvβ2 subunit far removed from the immediate site of contact with the α subunit. Together with the T1 domains, the $\alpha_4\beta_4$ complex would be expected to protrude as much as ~80 Å into the cytoplasm (Fig. 4B). Hence, it may be that the Kvβ2 tetramer acts as a molecular 'extension' of the α subunits into the cytoplasm, providing specific docking sites for additional regulatory factors to act on potassium channel.

Recent evidence suggests the existence of signaling complexes containing both ion channels and closely associated protein kinases and phosphatases [26–31]. Such ion channel-kinase/phosphatase complexes are thought to provide the necessary macromolecular organization for signaling specificity and regulation (for a recent review, see [32]). Purification of Kvβ2 subunit and imaging its oligomeric structure could provide a starting point to learn more about the stoichiometry and geometry of fully assembled potassium channels, which appear to be large, multicomponent complexes containing not

only α and β subunits, but also other associated proteins such as those typically involved in signal transduction pathways.

Acknowledgements: We thank Dr. A.P. Somlyo for use of his equipment, members of the Li laboratory for helpful comments on the manuscript, and Robyne Butzner for assistance with manuscript preparation. This work is supported by grants (to M.L.) from the National Institutes of Health (NS 33324), the A. Sloan Foundation and the J. Klingenstein Foundation. M.L. is an AHA-Pfizer Awardee. Z.S. is supported by grants from the National Institutes of Health (RR07720, HL48807) and from the American Heart Association. R.v.H. is supported in part by a postdoctoral fellowship from the American Heart Association.

References

[1] Doyle, D.A., Morais Cabral, J., Pfuetzner, R.A., Kuo, A., Gulbis, J.M., Cohen, S.L., Chait, B.T. and MacKinnon, R. (1998) Science 280, 69–77.
[2] Unwin, N. (1995) Nature 373, 37–43.
[3] Isom, L.L., De Jongh, K.S. and Catterall, W.A. (1994) Neuron 12, 1183–1194.
[4] Trimmer, J.S. (1998) Curr. Opin. Neurobiol. 8, 370–374.
[5] Xu, J. and Li, M. (1998) Trends Cardiovasc. Med. 8, 229–234.
[6] Jan, L.Y. and Jan, Y.N. (1992) Annu. Rev. Physiol. 54, 537–555.
[7] Miller, C. (1991) Science 252, 1092–1096.
[8] Rettig, J., Heinemann, S.H., Wunder, F., Lorra, C., Parcej, D.N., Dolly, J.O. and Pongs, O. (1994) Nature 369, 289–294.
[9] Shi, G., Nakahira, K., Hammond, S., Rhodes, K.J., Schechter, L.E. and Trimmer, J.S. (1996) Neuron 16, 843–852.
[10] Chouinard, S.W., Wilson, G.F., Schlimgen, A.K. and Ganetzky, B. (1995) Proc. Natl. Acad. Sci. USA 92, 6763–6767.
[11] MacKinnon, R. (1991) Nature 350, 232–235.
[12] Li, M., Unwin, N., Stauffer, K.A., Jan, Y.N. and Jan, L.Y. (1994) Curr. Biol. 4, 110–115.
[13] Li, M., Jan, Y.N. and Jan, L.Y. (1992) Science 257, 1225–1230.
[14] Xu, J., Yu, W., Jan, Y.N., Jan, L.Y. and Li, M. (1995) J. Biol. Chem. 270, 24761–24768.
[15] Shen, N.V., Chen, X., Boyer, M.M. and Pfaffinger, P.J. (1993) Neuron 11, 67–76.
[16] Yu, W.F., Xu, J. and Li, M. (1996) Neuron 16, 441–453.
[17] Sewing, S., Roeper, J. and Pongs, O. (1996) Neuron 16, 455–463.
[18] Kreusch, A., Pfaffinger, P.J., Stevens, C.F. and Choe, S. (1998) Nature 392, 945–948.
[19] Xu, J. and Li, M. (1997) J. Biol. Chem. 272, 11728–11735.
[20] Xu, J., Yu, W., Wright, J., Raab, R. and Li, M. (1998) Proc. Natl. Acad. Sci. USA 95, 1846–1851.
[21] Czajkowsky, D.M. and Shao, Z. (1998) FEBS Lett. 430, 51–54.
[22] Mou, J., Yang, J. and Shao, Z. (1995) J. Mol. Biol. 248, 507–512.
[23] Parcej, D.N., Scott, V.E. and Dolly, J.O. (1992) Biochemistry 31, 11084–11088.
[24] Popot, J.L. and Changeux, J.P. (1984) Physiol. Rev. 64, 1162–1239.
[25] Engel, A., Lyubchenko, Y. and Muller, D. (1999) Trends Cell Biol. 9, 77–80.
[26] Chung, S.K., Reinhart, P.H., Martin, B.L., Brautigan, D. and Levitan, I.B. (1991) Science 253, 560–562.
[27] Bielefeldt, K. and Jackson, M.B. (1994) Biophys. J. 66, 1904–1914.
[28] Rosenmund, C., Carr, D.W., Bergeson, S.E., Nilaver, G., Scott, J.D. and Westbrook, G.L. (1994) Nature 368, 853–856.
[29] Swope, S.L. and Huganir, R.L. (1994) J. Biol. Chem. 269, 29817–29824.
[30] Reinhart, P.H. and Levitan, I.B. (1995) J. Neurosci. 15, 4572–4579.
[31] Rotin, D., Bar-Sagi, D., O'Brodovich, H., Merilainen, J., Lehto, V.P., Canessa, C.M., Rossier, B.C. and Downey, G.P. (1994) EMBO J. 13, 4440–4450.
[32] Pawson, T. and Scott, J.D. (1997) Science 278, 2075–2080.
[33] Gulbis, J.M., Mann, S. and MacKinnon, R. (1999) Cell 97, 943–952.